Estuaries and Coasts
DOI 10.1007/s12237-012-9572-1

Environmental Controls on Net Ecosystem CO_2 Exchange Over a Reed (*Phragmites australis*) Wetland in the Yellow River Delta, China

Guangxuan Han · Liqiong Yang · Junbao Yu ·
Guangmei Wang · Peili Mao · Yongjun Gao

Received: 14 December 2011 / Revised: 6 May 2012 / Accepted: 14 May 2012

Abstract Using the Eddy Covariance (EC) technique, we analyzed temporal variation in net ecosystem CO_2 exchange (NEE) and determined the effects of environmental factors on the balance between ecosystem photosynthesis and respiration in a reed (*Phragmites australis*) wetland in the Yellow River Delta, China. Our results indicated that diurnal and seasonal patterns of NEE and its components (ecosystem respiration (R_{eco}), gross primary production (GPP)) varied markedly among months for the growing season (May to October). The cumulative CO_2 emission was 1,657 g CO_2 m^{-2}, while 2,612 g CO_2 m^{-2} was approximately accumulated as GPP, which resulted in the reed wetland being a net sink of 956 g CO_2 m^{-2}. The ratio of R_{eco} to GPP in reed wetland was 0.68, which was close to other temperate wetlands. Soil temperature and soil moisture exerted the primary controls on R_{eco} during the growing season. Daytime NEE values during the growing season were strongly correlated with photosynthetically active radiation. Aboveground biomass showed significant linear relationships with 24-h average NEE, daytime GPP, and R_{eco}, respectively. Thus, we conclude that the coastal wetland acted as a carbon sink during the growing season despite the variations in environmental conditions, and long-term flux measurements over these ecosystems are undoubtedly necessary.

Keywords Net ecosystem CO_2 exchange · Eddy covariance · Coastal wetlands · Environmental control · Yellow River Delta

Introduction

Wetlands play an important role in the global carbon cycle because they are among the most productive ecosystems in the world (Dušek et al. 2009; Schedlbauer et al. 2010). In particular, incomplete decomposition of organic material results in the accumulation of carbon and nutrients in most wetlands, covering about 15 % of the terrestrial organic carbon storage in the earth (Wickland et al. 2001; Sabine et al. 2004). Thus, the development of wetlands can affect the global climate system by reducing the concentration of CO_2 in the atmosphere (e.g., Dušek et al. 2009; Zhao et al. 2010). However, climate changes such as temperature increases and precipitation decreases may accelerate the decomposition rates in some wetlands, causing them to become net source of CO_2 to the atmosphere (Oechel et al. 1993; Nieveen et al. 1998). Therefore, it is important to investigate the carbon budget and its controlling mechanisms over different wetland ecosystems for accurately evaluating global carbon budgets and scientifically managing wetland ecosystems (Wickland et al. 2001; Zhou et al. 2009).

The net ecosystem CO_2 exchange (NEE) between an ecosystem and the atmosphere is the net balance of gross primary production (GPP) and total ecosystem respiration (R_{eco}). The EC technique has been widely used for quantifying NEE between the atmosphere and plant canopies in various wetland ecosystems (e.g., Bonneville et al. 2008; Zhou et al. 2009;

G. Han · L. Yang · J. Yu (✉) · G. Wang · P. Mao
Key Laboratory of Coastal Environment Processes, Yantai Institute of Coastal Zone Research, Chinese Academy of Sciences,
Chunhui Road 17, Laishan District,
Yantai, Shandong 264003, China
e-mail: jbyu@yic.ac.cn

L. Yang
Graduate University of Chinese Academy of Sciences,
Yuquan Road,
Beijing 100049, China

Y. Gao
Department of Earth and Atmospheric Sciences,
University of Houston,
Houston 77204-5007 TX, USA

Zhao et al. 2010), since it has the advantage that it is non-invasive, and that it can provide continuous, long-term flux information integrated at the ecosystem scale (Baldocchi 2003). The NEE varies substantially in space and time depending on the wetland's chemical, biological, and physical characteristics (Bonneville et al. 2008). Like all terrestrial ecosystems, a number of environmental factors can play important roles in governing the rate of NEE in wetlands. For example, previous studies have shown that temperature, light, water table depth, biomass, and leaf area index (LAI), and mineral nutrient characteristics of soil mostly controlled the dynamics of NEE in wetland (Syed et al. 2006; Bonneville et al. 2008; Zhou et al. 2009; Zhao et al. 2010). Bonneville et al. (2008) reported that during the growing season, variations of NEE were well correlated with variations in live biomass (r= 0.92) and green LAI (r=0.94) in a temperate cattail marsh wetland. Zhou et al. (2009) showed that daytime variation in NEE was strongly affected by the diurnal course of photosynthetically active radiation (PAR), and ecosystem respiration relied on temperature and soil water content in a reed wetland in Northeast China. Finally, light and air temperature exerted the primary controls on NEE in a short-hydroperiod Florida Everglades marsh during the dry season (Schedlbauer et al. 2010).

In recent years, most of EC studies of CO_2 exchange in wetlands have focused largely on peatlands and other temperate wetlands (e.g., Heikkinen et al. 2002; Syed et al. 2006; Bonneville et al. 2008; Zhao et al. 2010). There has been relatively few direct measurement of the CO_2 exchange between the atmosphere and coastal wetlands, regardless of their importance in balancing the global carbon budget and conserving biological diversity (Yan et al. 2008; Zhou et al. 2009). The Yellow River Delta is the fastest growing delta in the world, and the wetland of the Yellow River Delta is not only the most complete estuarine wetland, but also the youngest wetland ecosystem in the warm-temperate zone in China (Li et al. 2009). As a newly formed estuarine delta, it is naturally characterized by extensive coverage of primary salinization, which is mainly due to the presence of a shallow, saline water table and marine sediments (Guan et al. 2001; Zhang et al. 2011). Soil salt content is an important factor to halarch succession and vegetation distribution of the Yellow River Delta (Zhang et al. 2007). To date we have not found any relevant published studies on NEE over the coastal wetlands in the Yellow River Delta. Using the EC technique, the carbon fluxes in the growing season (May to October) of 2010 were measured over a reed (*Phragmites australis*) wetland in the Yellow River Delta, China. The objectives are (1) to determine the diurnal and seasonal variation of CO_2 exchange and calculate the carbon balance during the growing season for the ecosystem, (2) to identify the environmental controls of CO_2 exchange over the coastal wetland, and (3) to compare the ecosystem CO_2 exchange of the reed wetland with that of other coastal and inland wetlands.

Materials and Methods

Study Site Descriptions

The study was conducted in a reed ecosystem located on Yellow River Delta Ecological Research Station of Coastal Wetland (37°45′50″N, 118°59′24″E), which belongs to Yantai Institute of Coastal Zone Research, Chinese Academy of Sciences. The flux tower is located about 3 km south of the Yellow River channel, and about 20 km southwest of the mouth of the Yellow River (Fig. 1). The original vegetation of the Yellow River Delta is composed of halophytic plant communities predominated by herb and shrub species, such as *P. australis*, *Suaeda heteroptera*, and *Imperata cylindrical*. The terrain of the station is quite flat, with relatively homogeneous vegetation dominated by reed (*P. australis*), which usually bud during the end of March and the first 10 days of April, and head in the middle 10 days of October (Xie et al. 2011). The maximum canopy height at the peak of the growing season (early July to mid-August) can reach up to 1.50 m. During the rainy season (mid-July to mid-August), surface ponding (often less than 5 cm) was often observed in *P. australis* community, following heavy rainfall events, for time periods of less than 10 days.

The experimental site has a warm-temperate and continental monsoon climate with distinctive seasons and rainy summer. The annual average temperature is 12.9 °C ranging from 41.9 °C in the summer down to −23.3 °C in the winter. The average annual precipitation is 550–640 mm, with nearly 70 % of the precipitation falling between May and September, evaporation is 1,962 mm, and the drought index is up to 3.56. The mean annual wind speed is 2.98 ms^{-1}, and the frost-free period is 142 days (Xie et al. 2011). Generally, the soil type in the Yellow River Delta gradually varies from fluvo-aquic to saline soil, and the soil texture is mainly sandy clay loam. The prevailing wind directions in the 2010 growing season were from the north-east to the south-east (Fig. 2).

Meteorological and Aboveground Biomass Measurements

Meteorological parameters were measured with an array of sensors, including net radiation (CNR4, Kipp & Zonen USA Inc., Bohemia, NY, USA), PAR (LI-190SB, Li-Cor Inc., USA), air temperature (HMP45C, Vaisala, Helsinki, Finland), wind speed and direction (034B, Campbell Scientific Inc., USA), and precipitation (TE525 tipping bucket gauge, Texas Electronics, Texas, USA). Soil temperature was measured with thermistors (109SS, Campbell Scientific Inc., USA) at 5, 10, 30, and 50 cm depths below

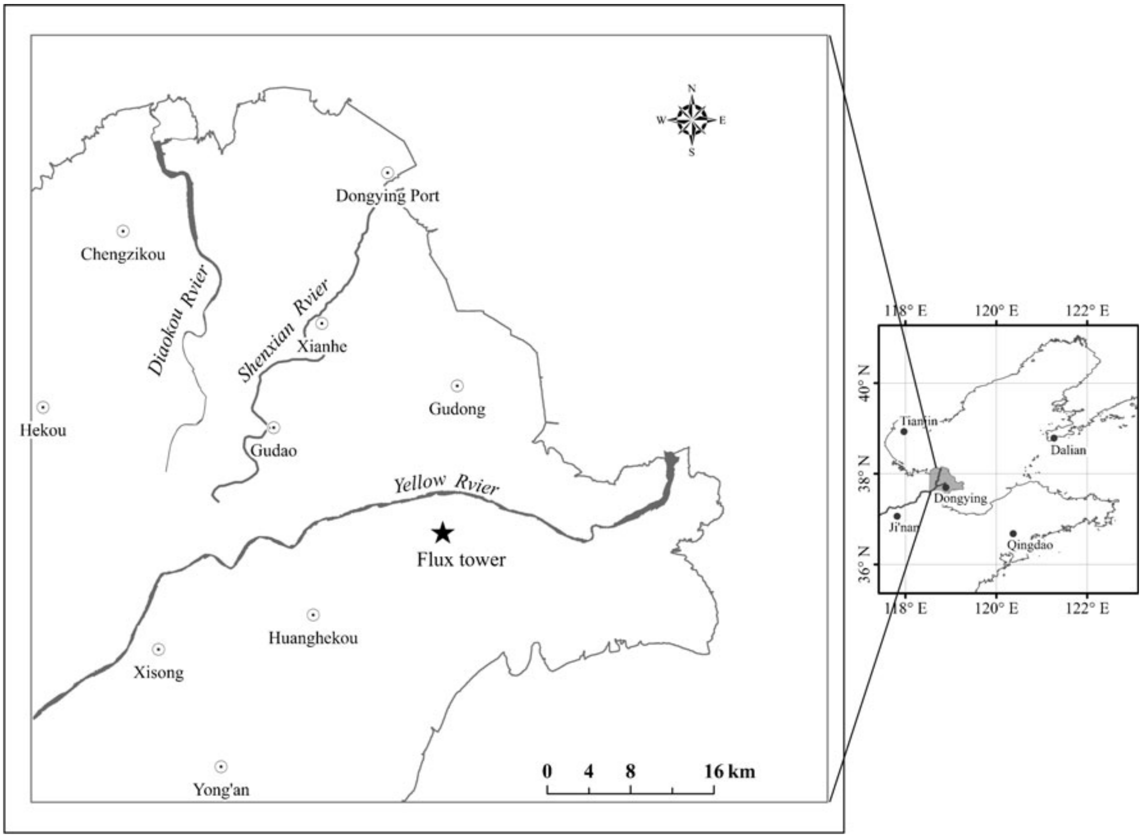

Fig. 1 Map of the Yellow River Delta and the location of flux tower

the surface. Soil water content was measured by time domain reflectometry probes (EnviroSMART SDI-12, Sentek Pty Ltd., USA) at 5, 10, 20, 40, 60, 80, and 100 cm depths below the surface. A data logger (Campbell Scientific Inc., USA) was used to collect these micrometeorological data. Variables measured every 15 s and averaged every 30 min for use in further analyses. During the growing season of 2010 (from May to October), the aboveground biomass of *P. australis* was measured by harvesting the vegetation approximately every 2 weeks. Five 0.5×0.5-m squares were randomly chosen within a radius of 200 m around the observation tower. Live plants were clipped at 1 cm above the ground level. Plant aboveground biomass was oven dried at 80 °C for 48 h and weighed.

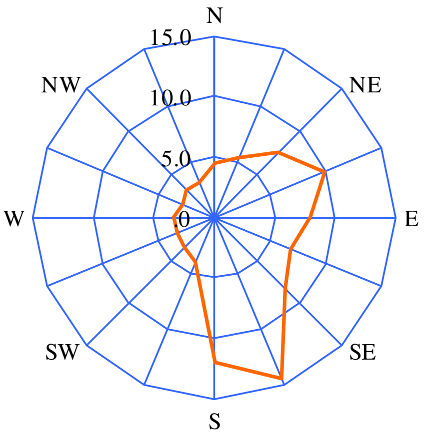

Fig. 2 Prevailing wind directions during the growing season in 2010 over a reed (*P. australis*) wetland in the Yellow River Delta, China

EC Measurements

The EC method has proven to be a valuable direct measurement of net carbon and water fluxes between ecosystems and the atmosphere (Falge et al. 2001; Baldocchi 2003). CO_2 flux of the reed wetland was calculated as the mean covariance of vertical wind velocity and scalar fluctuations, with the appropriate corrections applied (Syed et al. 2006). The following equation presents the calculation of CO_2 flux (Baldocchi 2003).

$$F_{CO_2} = \overline{\rho}_a \cdot \overline{\omega' c'} \quad (1)$$

where $\overline{\rho}_a$ is density of the air, ω' and c' are vertical wind speed and CO_2 concentration fluctuations from the means, respectively. Overbars in the equation show time averaging and primes represent fluctuations from mean value. Negative CO_2 flux represents CO_2 uptake by vegetation and positive flux represents CO_2 transfer into the atmosphere.

Continuous measurements of CO_2 flux data reported here began in May 2010 and continued through the end of the growing season in October 2010. CO_2 flux was measured by the EC method with a three-axis sonic anemometer (CSAT-3, Campbell Scientific Inc., USA) and open path infrared gas analyzer (IRGA, LI-7500, Li-COR Inc., USA), which were mounted 2.8 m above the ground on the tower in the center of the reed wetland (Fig. 1). Calculations with a footprint model (Hsieh et al. 2000) indicated that approximately 90 % of the cumulative flux footprint within 200 m upwind of the tower. The fetch from all directions is more than 300 m, so most of the measured fluxes came from the *P. australis* community. EC data were collected at 10 Hz on a CR1000 datalogger (Campbell Scientific Inc., USA) and stored on 2-GB Compact Flash cards. The collected data were also computed online every 30 min and recorded by the data logger, then adjusted by the WPL (Webb, Pearman, and Leuning) density correction (Webb et al. 1980).

EC Data Processing and Quality Control

EC flux data could include erroneous data due to the affections of instrument malfunction, rainfall, human disturbance, and atmospheric conditions inappropriate for EC measurements (Saito et al. 2005; Alberto et al. 2009). Raw EC data collected from a Campbell Scientific datalogger were processed with EdiRe (v.1.4.3.1186) from the University of Edinburg (Scotland) to determine net ecosystem CO_2 exchange with an averaging period (30 min). Data processing followed standard methods and included despiking, coordinate rotation, time lag corrections, and air density corrections (Webb et al. 1980; Polsenaere et al. 2012).

In order to provide quality control of raw data by excluding data when there were rainfalls, dew formation, power failure, or equipment failure, we performed the tests for stationarity and integral turbulent characteristics. During stationarity tests, the procedure following Foken and Wichura (1996) was applied, with the rejection threshold set to 30 % (Guo et al. 2009). During integral turbulent tests, we utilized the test for $\sigma w/u^*$ (Kaimal and Finnigan 1994), where σw is the 30-min standard deviation of weed speed and u^* is the friction velocity. Values that varied by more than 30 % compared to the reference were rejected (Guo et al. 2009). Moreover, the following filtering algorithms were applied to half-hourly flux data for reducing the uncertainty of the data, including (1) precipitation or condensation on the IRGA or sonic anemometer, (2) biologically impossible values of NEE for the reed wetlands ($|\text{NEE}|>3$ mg CO_2 $m^{-2}s^{-1}$) (Zhou et al. 2009), (3) the flux data under weak turbulence (friction velocity, $u^*<0.15$ ms^{-1}), (4) excessive spikes in the sonic and IRGA data, (5) insufficient sample points ($N<15{,}000$) were collected during a 30-min period (Zhou et al. 2009; Schedlbauer et al. 2010).

It has been recognized that the EC technique is likely to underestimate the flux in stable conditions during the night, so most of the researchers screened the nighttime data on the basis of u^* threshold (Zhou et al. 2009; Schedlbauer et al. 2010). Below u^* values of 0.15 ms^{-1} a decreasing trend in the flux was observed (Fig. 3), suggesting an under-measurement of CO_2 exchange. Therefore, all half-hourly NEE data at night with $u^*\leq 0.15$ ms^{-1} were excluded from the dataset. The available flux data were more than 65 % of EC flux observation data.

Flux Gap Filling

We used the following procedure to fill missing and bad data. Small gaps (less than 2 h) were filled by linear interpolation. Large gaps (more than 2 h) were filled based on empirical models separately for daytime and nighttime data. When Rn was <10 Wm^{-2}, nighttime missing NEE data were filled with the exponential relationship between R_{eco} and soil temperature at 5-cm function (Lloyd and Taylor 1994):

$$R_{\text{eco}} = a\exp(bT_{\text{soil}}) \tag{2}$$

where R_{eco} is nighttime NEE (i.e., ecosystem respiration), T_{soil} is soil temperature at depth of 5 cm, *a* and *b* are two empirical coefficients.

Q_{10} can be estimated as

$$Q_{10} = \exp(10b) \tag{3}$$

When Rn was >10 Wm^{-2}, daytime NEE data were gap-filled using the Michaelis–Menten model (Ruimy et al. 1995; Falge et al. 2001),

$$\text{NEE} = -\frac{\text{A}_{\max}\alpha\text{PAR}}{\text{A}_{\max}+\alpha\text{PAR}} + \text{R}_{\text{eco}} \tag{4}$$

where the coefficient α is apparent quantum yield (milligrams of CO_2 per micromole of photon), A_{max} is light-saturated net CO_2 exchange (milligrams of CO_2 per square meter per second), and R_{eco} is daytime ecosystem respiration (milligrams of CO_2 per square meter per second).

Due to seasonal changes in plant biomass and meteorological conditions, the GPP-PAR and R_{eco}-T_{soil} relationships vary in time. Therefore, separate relationships in Eqs. (2) and (4) were derived monthly during the growing seasons. In cases where empirical relationships could not be developed as a result of missing meteorological data, mean diurnal variation was used to fill the gap (Falge et al. 2001).

NEE Partitioning into GPP and R_{eco}

NEE was partitioned into its components using the equation (Zhang et al. 2007; Alberto et al. 2009; Schedlbauer et al. 2010):

$$\text{NEE} = \text{R}_{\text{eco}} - \text{GPP} \tag{5}$$

where GPP represents CO_2 assimilation by photosynthesis of vegetation and R_{eco} represents the CO_2 released through respiration of soil and plants.

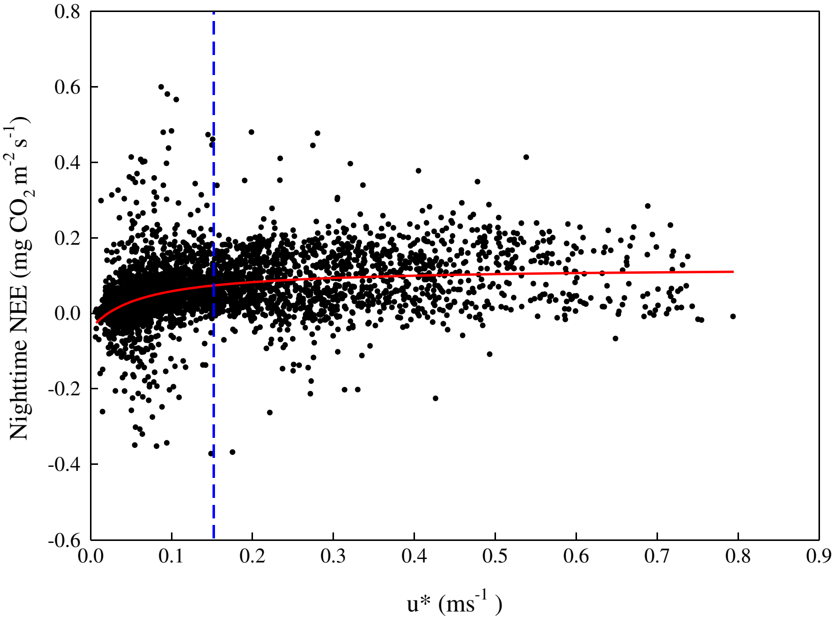

Fig. 3 Determination of the threshold friction velocity (u*) during the growing season (from May to October) in 2010. The *solid line* represents a smoothed function fitted to the data. The *dashed line* represents the threshold below which the flux is lower. The u* threshold for the site is 0.15 ms^{-1}

Direct measurement of GPP and R_{eco} is difficult because foliage light respiration is unknown. Therefore, R_{eco} could be firstly obtained by the exponential function (Eq. (2)), in order to separate diurnal NEE into photosynthetic and respiratory fluxes (Saito et al. 2005; Glenn et al. 2006; Alberto et al. 2009; Schedlbauer et al. 2010).

$$R_{eco} = R_{eco,day} + R_{eco,night} \tag{6}$$

where daily R_{eco} is the sum of daytime respiration ($R_{eco,day}$) and the nighttime respiration ($R_{eco,night}$).

Based on the assumption that $R_{eco,day}$ was of similar magnitude and responsiveness as $R_{eco,night}$, $R_{eco,day}$ was determined using the predictive relationships developed for nighttime periods (Falge et al. 2001; Alberto et al. 2009; Zhou et al. 2009; Schedlbauer et al. 2010). Then GPP was calculated as the residual between NEE and R_{eco}. Daily and monthly values of GPP and R_{eco} were summed from the half-hourly data (Zhou et al. 2009).

Results

Meteorological Conditions and Aboveground Biomass during the Growing Season

PAR fluctuations clearly indicated frequent cloudy conditions during growing season (Fig. 4a). Average monthly PAR reached its maximum in June (613.4 μmolm^{-2}s^{-1}) and July (619.2 μmol m^{-2}s^{-1}), and then decreased gradually (down to 188.7 μmolm^{-2} s^{-1} in October). The distribution of air temperature (Tair) showed a large variation and mean Tair was 21.4 °C with a daily maximum at 31.6 °C in July and a minimum at 5.2 °C in late October (Fig. 4b). The total rainfall during the 2010 growing season was 494.7 mm, with the largest daily rainfall of 78.9 mm occurred at 19 August (Fig. 4c). Seasonal fluctuations in temperature and rainfall affected soil water content (SWC). Seasonal variation of SWC in the top 10- and 20-cm soil layer displayed a similar pattern of changes, and they were related to the intensity and frequency of rainfall (Fig. 4c). Aboveground biomass of *P. australis* increased during the early growing season, and reached a maximum of 255.6 g DM m^{-2} during mid-August in 2010, followed by a steady decline as the community senesced (Fig. 4d).

Temporal Variations in CO$_2$ Exchange Flux

The daily GPP and R_{eco} of the reed wetland were very low during the early vegetative stage with an average of 6 g CO$_2$ m^{-2}day^{-1} (Fig. 4e). They showed rapid increase from late May with the reed growth, and reached a maximum absorption rate of 30 g CO$_2$ m^{-2}day^{-1} on 28 July and a maximum release rate of 18 g CO$_2$ m^{-2}day^{-1} on 31 July. Warmer temperatures and larger canopy size in June and July caused GPP and R_{eco} to increase. Then, the daily GPP and R_{eco} sharply decreased in fall (September through October). Seasonal NEE showed a distinct V-like course for the growing season (from May to October). The reed wetland acted as a slight source of CO$_2$ for the first 20 days of the growing period. The reed wetland started to become a sink for CO$_2$ in late May and the highest NEE was observed in July, due to less cloudiness and relatively high leaf area. It reached its maximum daily uptake of −16 g CO$_2$ m^{-2}day^{-1} on 11 July. From then on, NEE started to become less negative as GPP decreased, and it began to rise to positive in late September and October because of relatively cold temperature and defoliation of reed. However, very small values of NEE

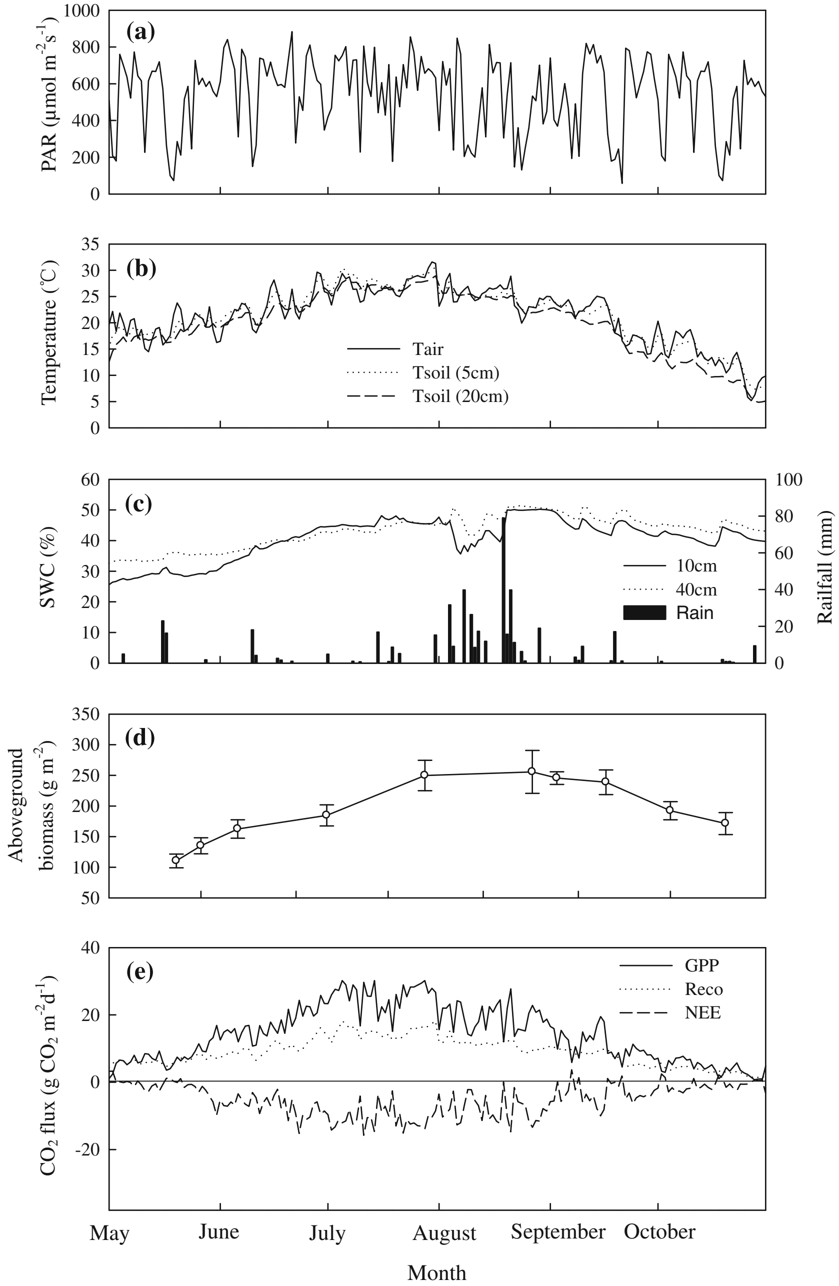

Fig. 4 Seasonal variations of environmental conditions, reed aboveground biomass, and CO_2 exchange in the 2010 growing season over a reed (*P. australis*) wetland in the Yellow River Delta, China, showing **a** daily photosynthetic available radiation (PAR), **b** 24-h mean air (2 m) and soil temperature (5 and 20 cm), **c** daily mean soil water content (*SWC*, 10 and 20 cm) and daily rain fall, **d** reed aboveground biomass, and **e** daily gross primary production (*GPP*), ecosystem respiration (R_{eco}), and net ecosystem exchange (*NEE*)

appeared occasionally in July and August. This always happened on cloudy days when soil temperature was high.

During the growing season, average NEE for each month was a CO_2 source (positive flux values) at night and a CO_2 sink (negative flux values) during the day (Fig. 5). After sunrise, the NEE moved from a positive value (release) to a negative value (uptake), and CO_2 uptake increased gradually till a peak was observed around noon. Then, CO_2 uptake declined rapidly through the afternoon, and turned to release of CO_2 immediately after sunset. During the early vegetative season, only a small net uptake of CO_2 (maximum absorption rate was −0.08±0.01 mg CO_2 $m^{-2}s^{-1}$) was observed during the daylight hours in May, with associated small net CO_2 losses (maximum release rate was 0.04±0.003 mg CO_2 $m^{-2}s^{-1}$) at night. The amplitude of the diurnal variation in NEE increased with reed growth, and the daily maximum CO_2 uptake values occurred during the peak growing seasons (July and August). The maximum uptake rates were −0.55±0.02 and -0.57±0.04 mg CO_2 $m^{-2}s^{-1}$ in July and August, respectively. Meanwhile, the nighttime release rates were 1.14±0.01 and 1.17±0.01 mg CO_2 $m^{-2}s^{-1}$ in July and August, respectively. With the decrease of air temperature and the defoliation of reed ecosystem, the decline in ecosystem CO_2 exchange began in September and very little diurnal variation was evident in NEE at the end of the vegetative season.

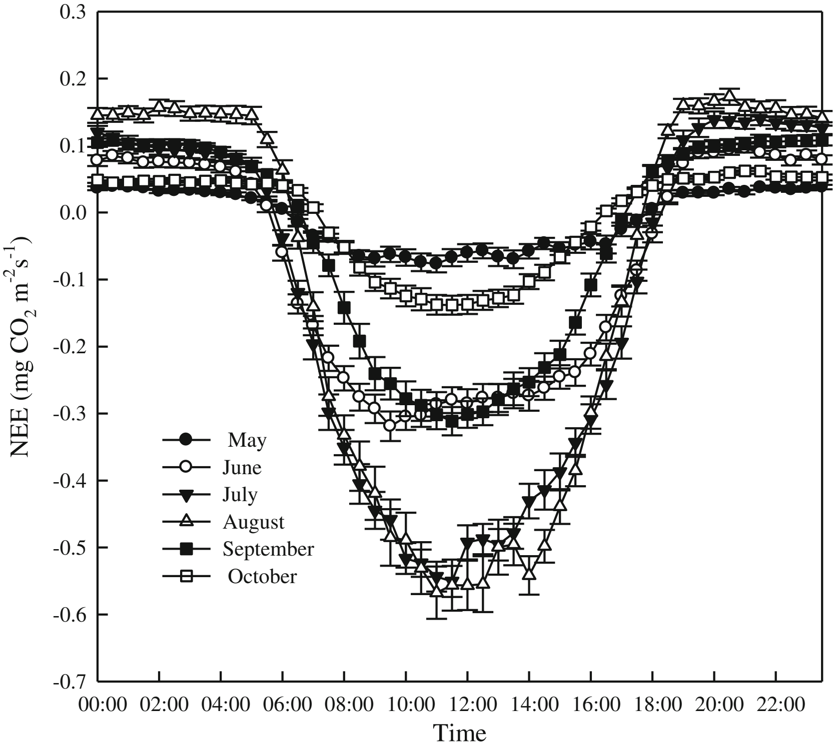

Fig. 5 Daily variations of net ecosystem CO_2 exchange (*NEE*) during May–October 2010 in a reed wetland. The NEE values for each month were binned by time of day and averaged. *Bars* represent standard errors of the means

Variation of Cumulative CO_2 Fluxes

Overall, the reed wetland absorbed carbon for 159 days during growing season of 2010 in the Yellow River Delta. During the growing season from May to October, the cumulative CO_2 emission sum was as high as 1,657 g CO_2 m^{-2}, while approximately 2,612 g CO_2 m^{-2} was accumulated as GPP, which resulted in the reed wetland being a net sink of 956 g CO_2 m^{-2} (monthly averages of −32, −210, −333, −251, −102, −27 g CO_2 m^{-2}, respectively; Table 1, Fig. 6).

Discussion

Effects of Soil Temperature and Moisture on Nighttime NEE

The most important environmental factors that affect R_{eco} are temperature and soil moisture (Buchmann 2000). Correlation analysis revealed that the nighttime NEE (R_{eco}) was more significantly related to soil temperature at 5-cm depth (r=0.86) and soil water content at 10-cm depth (r=0.55) than those at the other depths during the growing season (Table 2). Thus, soil temperature at 5-cm depth and soil water content at 10-cm depth were used to investigate the influence of temperature and moisture on R_{eco}. An exponential function relating R_{eco} to soil temperature accounted for approximately 68 % of variation in R_{eco} during the growing season in 2010 (Fig. 7a). Previous studies in other wetland ecosystems have shown that R_{eco} increased with increasing temperature (Alberto et al. 2009). For example, Zhou et al. (2009) reported that the relationships between R_{eco} and soil temperature were well fitted with an exponential function (r^2 ranged from 0.42 to 0.69) in a reed wetland in Northeast China. Hirota et al. (2006) demonstrated R_{eco} was exponentially correlated with soil temperature (5 cm), and soil temperature accounted for approximately 48–88 % of variation in R_{eco} in a deep-water wetland on the Qinghai-Tibetan Plateau. The exponential relationship between respiration and soil temperature results from the combined response of microbial and plant respiration to temperature (Wickland et al. 2001). Increasing temperatures can activate dormant microbes and increase microbial species richness and bacterial metabolism, which potentially broadened the mineralizable carbon pools (Andrews et al. 2000), thus promoting microbial respiration. At the same time, plant respiration is an environmentally sensitive component of the ecosystem carbon balance, and

Table 1 Comparison of the CO_2 flux (gram of CO_2 per square meter) from May to October in 2010 in the reed wetland

	May	June	July	August	September	October	Growing season
NEE	−32	−210	−333	−251	−102	−27	−956
GPP	229	518	801	599	334	131	2,612
R_{eco}	197	308	468	348	232	104	1,657
R_{eco}/GPP	0.86	0.59	0.58	0.58	0.69	0.79	0.68

Fig. 6 Cumulative carbon balance with the main components of the CO_2 exchange (*GPP*, R_{eco}, *NEE*) in a reed wetland from May to October in 2010

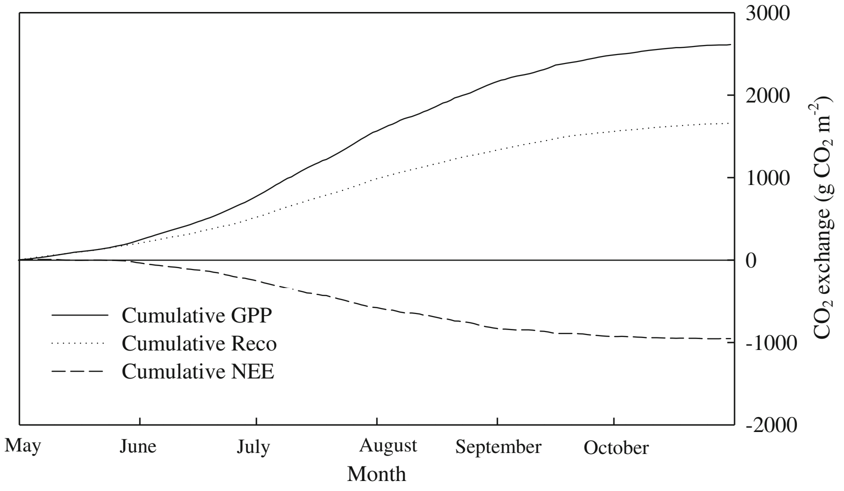

rates of the enzymatic processes of respiration increase with temperature (Ryan 1991).

Soil moisture is another important factor influencing ecosystem respiration. In order to assess the effect of soil moisture on ecosystem respiration, R_{eco} was plotted against the nighttime soil water content at 10-cm depth during the growing season (Fig. 7b). The relationship could be described by a quadratic equation. When the values of SWC ranged from 20 to 50 %, R_{eco} increased with increasing SWC, and about 32 % of the variation in R_{eco} was explained by changes in SWC. Evidence for the effect of soil moisture on R_{eco} comes from a series of recent studies. For instance, the CO_2 release rate seemed to increase linearly as soil water content increased in a reed wetland, and soil water content could explain 50 % of the variation of nighttime ecosystem respiration (Zhou et al. 2009). Alberto et al. (2009) also observed that soil moisture had important influence on R_{eco} in an aerobic rice field, and the relationship could be described by a quadratic equation. Therefore, the effects of temperature and moisture on Q_{10} are of critical importance in assessing the impacts of changing climate on ecosystem carbon fluxes (Zhang et al. 2007). Thus, we determined R_{eco} as an exponential function of T_{soil} under different SWC levels (Table 3). The result showed the higher Q_{10} appeared in relatively moderate soil moisture condition (30 %<SWC<40 %), and Q_{10} declined with reductions or increases in soil moisture.

Several mechanisms were responsible for higher Q_{10} occurring at an intermediate soil moisture level. Firstly, soil drought restricted autotrophic respiration and soil heterotrophic respiration by decreasing biological activity or substrate availability (Van Dijk and Dolman 2004; Shi et al. 2006). It has been found empirically that Q_{10} values decrease with declining soil moisture status (Reichstein et al. 2002). Secondly, the high soil moisture could impede oxygen diffusion into the soil (Xu and Qi 2001), thereby reducing the soil respiration rate and affecting the Q_{10} value of ecosystem respiration. Last, but not least, the higher Q_{10} values for intermediate soil moisture might be related to the fact that these data often represented June, July, and August (Fig. 4), which were the peak growing season of *P. australis* community. The phenological stage of plant growth and development may be one of the most important factors controlling the temperature sensitivity of soil respiration (DeForest et al., 2006), thereby affecting the Q_{10} value of ecosystem respiration. Our results clearly illustrate that soil moisture can also have an important influence on the Q_{10} value of ecosystem respiration, and the same results have been reported in other previous studies. Reichstein et al. (2002) reported a significant decline in Q_{10} (from 0.5 to 2.6) when the relative soil water content (fraction of field capacity) dropped from 1 to 0.4 for three Mediterranean evergreen sites. Flanagan and Johnson (2005) reported that Q_{10} declined with reductions in soil moisture in a northern temperate grassland. Thus, in modeling long-term ecosystem respiration, one should account for how Q_{10} varies over the season with changes in soil moisture, temperature, and phenology (Zhang et al. 2006).

Table 2 Correlation coefficients of R_{eco} to air and soil temperatures and soil water content in the reed wetland ecosystem of the Yellow River Delta

Temperature (°C)					Soil water content (%)				
Air	5-cm soil	10-cm soil	20-cm soil	30-cm soil	10 cm	20 cm	40 cm	60 cm	80 cm
0.85**	0. 86**	0.83**	0.80**	0.83**	0.55**	0.51**	−0.20**	0.12**	−0.05

**p<0.01; two tailed

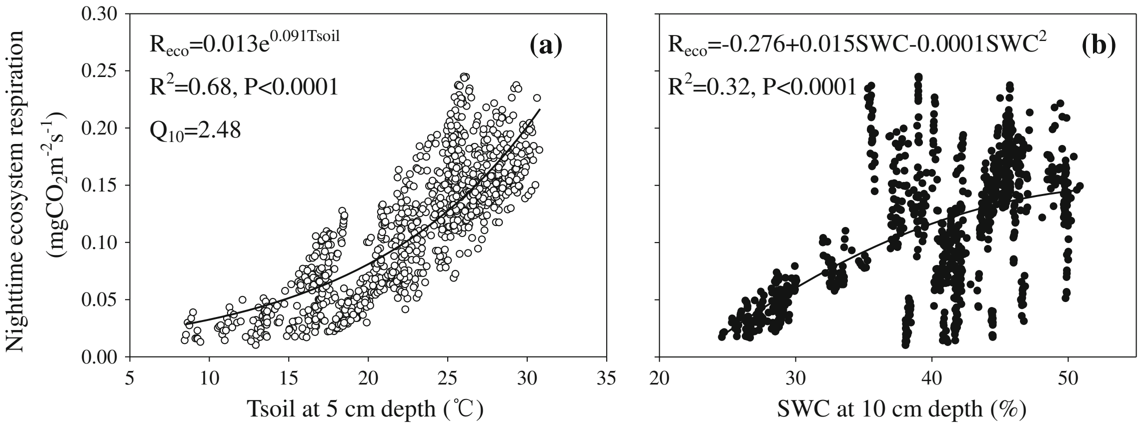

Fig. 7 Relationship between ecosystem respiration (R_{eco}) and soil temperature at 5-cm depth and soil water content (*SWC*) at 10-cm depth during the growing season in 2010. *Black lines* are the best fit exponential and quadratic relationships, respectively

Effects of PAR on Daytime NEE

The Michaelis–Menten model (Eq. (4)) appeared to be an appropriate model for modeling daytime NEE during different months of 2010 (Fig. 8). Daytime NEE increased with PAR at low-to-intermediate levels of PAR, but as PAR exceeded the light saturation point, NEE began to decline (Fig. 8). This threshold value of PAR is called the photosynthetic capacity (Ruimy et al. 1995). The decline indicates a decrease in light use efficiency, when photosynthetic photon flux density increases because of PAR saturation in the canopy (Arain and Restrepo-Coupe 2005). The seasonal variations of parameters estimated from the model, $A_{\max}$, α, and R_{eco}, could be represented as single peak curves (Table 4). These observations at this wetland were similar to those observed at other wetland ecosystems of Glenn et al. (2006), Syed et al. (2006), and Zhou et al. (2009), which reported the seasonal variations of parameters represented as single peak curves.

The peak values of $A_{\max}$ were observed in August at about 0.63 mg CO_2 $m^{-2}s^{-1}$, which was caused by large PAR, high air and soil temperature, and large canopy size. Variation of $A_{\max}$ among different growth periods could be caused by changes in plant growth, and environmental conditions (Zhou et al. 2009). Saito et al. (2005) reported $A_{\max}$ showed the increase with the increase of LAI and reached a maximum around the heading period (24–31 July) in rice paddy field in Japan. Zhou et al. (2009) reported temperature could explain 60–80 % of the seasonal variation of $A_{\max}$ in a reed wetland. The quantum yield α followed the same pattern ranging from 0.0013 to 0.0042 mg CO_2 μmol^{-1} photon, which was close to an estuarine wetland (from 0.004 to 0.0038 mg CO_2 μmol^{-1} photon) in coastal Shanghai (Guo et al. 2009) and smaller than other EC studies in reed wetland ecosystems (e.g., Zhou et al. 2009). Small canopy size and low temperature at early season resulted in the low α (Xu and Baldocchi 2004), and increased

Table 3 Relationship between R_{eco} and T_{soil} under different SWC in the reed wetland ecosystem ($P<0.01$)

SWC levels	Respiration–temperature relationship	*n*	r^2	Q_{10}
≤30 %	$y=0.003e^{0.124x}$	137	0.55	3.5
30 %<SWC≤40 %	$y=0.005e^{0.137x}$	205	0.63	3.9
40 %<SWC≤45 %	$y=0.014e^{0.087x}$	332	0.57	2.4
45 %<SWC≤55 %	$y=0.013e^{0.091x}$	259	0.56	2.5

y ecosystem respiration (milligram of CO_2 per square meter per second), *x* 5-cm soil temperature (degrees Celsius)

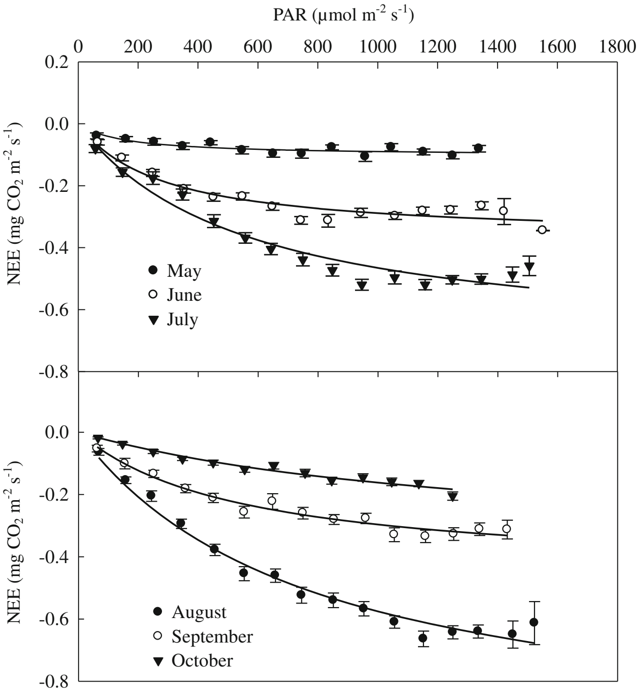

Fig. 8 Relationship between net ecosystem CO_2 exchange (*NEE*) and photosynthetic photon flux (*PAR*) during May–October 2010 in a reed wetland. The *curves* are nonlinear least squares fits of the Michaelis–Menten model (Eq.(4)). The daytime NEE data were averaged with PAR bin of a width of 100 μmolm^{-2}s^{-1}

Table 4 Comparison of parameters of relationship between net ecosystem CO_2 exchange and photosynthetic photon flux using a Michaelis–Menten model (Eq. (4))

Month	A_{max}	α	R_{eco}	n	r^2
May	−0.07	0.0013	0.03	14	0.70
June	−0.33	0.0017	0.17	16	0.57
July	−0.55	0.0032	0.22	16	0.67
August	−0.63	0.0042	0.25	16	0.75
September	−0.34	0.0022	0.14	15	0.77
October	−0.26	0.0018	0.04	13	0.92

n number of observations, R_{eco} ecosystem respiration (milligram of CO_2 per square meter per second), A_{max} maximum ecosystem photosynthetic assimilation (milligram of CO_2 per square meter per second); α: ecosystem quantum yield (milligram of CO_2 per micromole of photon), r^2 squared correlation coefficient of the fit

$P<0.01$

with plant growth and increasing temperature. Dark respiration (R_{eco}) calculated from the Michaelis–Menten equation (Eq. (4)) was in the range 0.03 to 0.25 mg CO_2 $m^{-2}s^{-1}$. Dark respiration changed as plant growth and temperature because of its link to photosynthesis.

Effects of Aboveground Biomass on the CO_2 Flux

During the growing season, aboveground biomass showed significant linear relationships with 24-h average NEE (measured on biomass sampling date; $r^2=0.87$, $n=9$, $P<0.001$), daytime GPP ($r^2=0.83$, $n=9$, $P<0.001$), and R_{eco} ($r^2=0.70$, $n=9$, $P<0.001$), respectively (Fig. 9), suggesting the increase in the absolute magnitudes of GPP, R_{eco}, NEE were associated with an increase of aboveground plant biomass (Fig. 4d, e). Our results are consistent with those in previous findings (Heikkinen et al. 2002; Hirota et al. 2006), which showed that GPP, R_{eco}, and NEE revealed significant linear correlations with the temporal variation in aboveground biomass. On the one hand, aboveground respiration contributed significantly to R_{eco} and therefore the variation in the amount of aboveground biomass modulated the variability in R_{eco} (Wohlfahrt et al. 2008). On the other hand, aboveground biomass reflected the photosynthetic capacity of the stand, the seasonal NEE is related to the amount of carbon accumulated in plant biomass (Larmola et al. 2003). Thirdly, aboveground biomass correlated with LAI (Wickland et al. 2001), which resulted in light use efficiency during the early (May) and late (September and October) lower than that during the middle of the growing season (June to August). Finally, the increase in aboveground production implied an increase in total root carbon allocation, thus enhanced root respiration and R_{eco} (Högberg et al. 2002; Curiel-Yuste et al. 2004).

Comparison with Other Wetland Ecosystems

Recent studies of carbon sequestration by coastal and estuarine wetlands have brought basic information about their seasonal dynamics of NEE. The growing season (May–October) carbon budgets determined in this study is lower than the average net carbon uptake of a reed estuarine wetland (1,437 g CO_2 m^{-2}) in Northeast China (Zhou et al. 2009), an estuarine wetland (1,181 g CO_2 m^{-2}) on Chongming Island, Shanghai (Yan et al. 2010), and higher than that of a coastal marsh (477 g CO_2 m^{-2}) in North American Atlantic (Kathilankal et al. 2008). Luo and Xing (2010) found that average soil respiration rate of the reed wetland in the Yellow River Estuary was 0.05 mg CO_2 $m^{-2}s^{-1}$ in May. In our study, the R_{eco} of the ecosystem in May was 0.07 mg CO_2 $m^{-2}s^{-1}$. Thus, soil respiration in May was estimated to contribute 71 % of the total R_{eco} in the reed wetland. On the other hand, compared with other inland wetlands, the net CO_2 exchange of the coastal wetland in Yellow River Delta is comparable to values reported for a temperate cattail marsh (Bonneville et al.

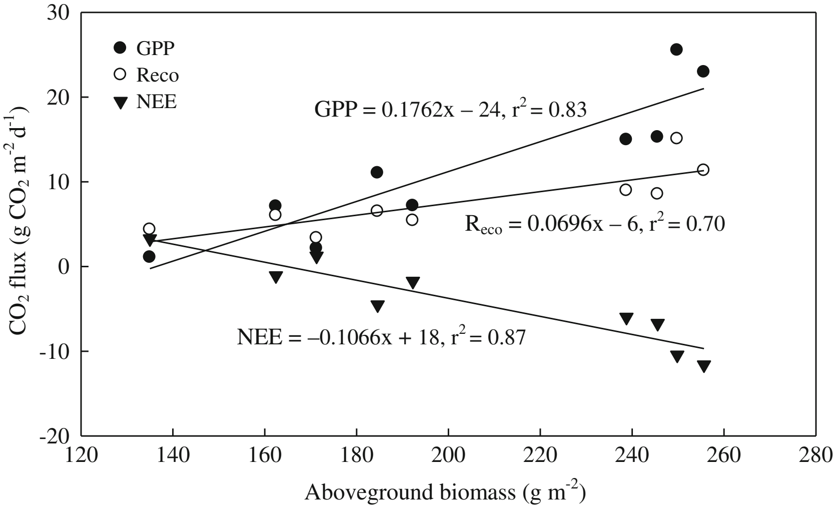

Fig. 9 Linear relationships between the main components of the CO_2 exchange (*GPP*, R_{eco}, and *NEE*) and aboveground biomass of reed (*P. australis*) from May to October in 2010

2008) and for a salt marsh (Houghton and Woodwell 1980). However, it is higher than that of a wet lawn tundra wetland (165 g CO_2 m^{-2}) in Northeast Europe (Heikkinen et al. 2002), a boreal oligotrophic pine fen (396 g CO_2 m^{-2}) in Finland (Alm et al. 1997) and a deep-water wetland (324 g CO_2 m^{-2}) on the Qinghai-Tibetan Plateau (Hirota et al. 2006) for the growing season. In addition, the ratio of R_{eco} to GPP could be used to evaluate the relative contribution of carbon exchange processes (respiration and photosynthesis) to total annual exchange (Falge et al. 2001). In our study, the ratio of R_{eco} to GPP in reed wetland was 0.68 during the growing season (Table 1), which was close to an poor fen (0.7) in northern Alberta (Glenn et al. 2006), an wet lawn tundra wetland (0.72) in Northeast Europe (Heikkinen et al. 2002) and a boreal oligotrophic pine fen (0.65) in Finland (Alm et al. 1997) for the growing season.

Although the coastal wetland in this study was a significant CO_2 sink during the growing season of 2010, on an annual basis it could be a net CO_2 source, due to negative NEE during the rest of the year. In addition, the wetlands still likely increase the greenhouse effect because they also showed a shift from a net CO_2 sink to a large source probably caused by environmental factors (Oechel et al. 1993; Nieveen et al. 1998; Syed et al. 2006). For example, on the Texas Gulf Coast, a high marsh was a net CO_2 sink (−7 g CO_2 $m^{-2}day^{-1}$) during periods of high water availability and low sediment salinity, and a net source (9 g CO_2 $m^{-2}day^{-1}$) when water availability was low and salinity was high (Heinsch et al. 2004). Thus, this emphasizes the scientific need for long-term and continuous measurements of CO_2 exchange in various wetland ecosystems (Nieveen et al. 1998).

Conclusions

The diurnal and seasonal patterns of NEE and its components (R_{eco}, GPP) varied markedly among months for the growing season over the reed wetland in the Yellow River Delta, China. Over the 6-month growing season, the reed wetland was acting as a net sink of 956 g CO_2 m^{-2}. The ratio of R_{eco} to GPP in reed wetland was 0.68. Environmental factors exerted major controls on the carbon balance of reed wetland at multiple temporal scales. Soil temperature and soil moisture exerted the primary controls on R_{eco}. Daytime NEE values during the growing season were strongly correlated with PAR. Aboveground biomass showed significant linear relationships with 24-h average NEE, daytime GPP and R_{eco}, respectively. These results would improve knowledge of CO_2 exchange dynamics over reed wetland ecosystem and aid in the prediction of future coastal ecosystem responses to environmental factors change.

Acknowledgments This research was funded by the National Science and Technology Support Program of China (No. 2011BAC02B01), the Chinese Academy of Sciences (no. kzcx2-yw-223), the CAS/SAFEA International Partnership Program for Creative Research Teams (Representative environmental processes and resources effects in coastal zone), and the 100 Talents Program of the Chinese Academy of Sciences. We also thank Dr. Yuhong Liu, Xiaobing Chen, Baohua Xie, and two anonymous reviewers for their expert advice and fruitful comments.

References

Alberto, M.C.R., R. Wassmann, T. Hirano, A. Miyata, K. Arvind, A. Padre, and M. Amante. 2009. CO_2/heat fluxes in rice fields: comparative assessment of flooded and non-flooded fields in the Philippines. *Agricultural and Forest Meteorology* 149: 1737–1750.

Alm, J., A.V. Talanov, S. Saarnio, J. Silvola, E. Ikkonen, H. Aaltonen, H. Nykänen, and P.J. Martikainen. 1997. Reconstruction of the carbon balance for microsites in a boreal oligotrophic pine fen, Finland. *Oecologia* 110: 423–431.

Andrews, J.A., R. Matamala, K.M. Westover, and W. Schlesinger. 2000. Temperature effects on the diversity of soil heterotrophs and the $\delta^{13}C$ of soil-respired CO_2. *Soil Biology Biochemistry* 32: 699–706.

Arain, M.A., and N. Restrepo-Coupe. 2005. Net ecosystem production in a temperate pine plantation in southeastern Canada. *Agricultural and Forest Meteorology* 128: 223–241.

Baldocchi, D.D. 2003. Assessing the eddy covariance technique for evaluating carbon dioxide exchange rates of ecosystems: past, present and future. *Global Change Biology* 9: 479–492.

Bonneville, M.C., I.B. Strachan, E.R. Humphreys, and N.T. Roulet. 2008. Net ecosystem CO_2 exchange in a temperate cattail marsh in relation to biophysical properties. *Agricultural and Forest Meteorology* 148: 69–81.

Buchmann, N. 2000. Biotic and abiotic factors controlling soil respiration rates in Picea abies stands. *Soil Biology and Biochemistry* 32: 1625–1635.

Curiel-Yuste, J., I.A. Janssens, A. Carrara, and R. Ceulemans. 2004. Annual Q_{10} of soil respiration reflects plant phonological patterns as well as temperature sensitivity. *Global Change Biology* 10: 161–169.

DeForest, J.L., A. Noormets, S. McNulty, G. Tenney, G. Sun, and J. Chen. 2006. Phenophases alter the soil respiration-temperature relationship in an oak-dominated forest. *International Journal of Biometeorology* 51: 135–144.

Dušek, J., H. Čížková, R. Czerný, K. Taufarová, M. Šmídová, and D. Janouš. 2009. Influence of summer flood on the net ecosystem exchange of CO_2 in a temperate sedge-grass marsh. *Agricultural and Forest Meteorology* 149: 1524–1530.

Falge, E., D. Baldocchi, R.J. Olson, P. Anthoni, M. Aubinet, C. Bernhofer, G. Burba, R. Ceulemans, R. Clement, H. Dolman, A. Granier, P. Gross, T. Grünwald, D. Hollinger, N.-O. Jensen, G. Katul, P. Keronen, A. Kowalski, C. Ta Lai, B.E. Law, T. Meyers, J. Moncrieff, E. Moors, J.W. Munger, K. Pilegaard, Ü. Rannik, C. Rebmann, A. Suyker, J. Tenhunen, K. Tu, S. Verma, T. Vesala, K. Wilson, and S. Wofsy. 2001. Gap filling strategies for defensible annual sums of net ecosystem exchange. *Agricultural and Forest Meteorology* 107: 43–69.

Flanagan, L.B., and B.G. Johnson. 2005. Interacting effects of temperature, soil moisture and plant biomass production on ecosystem respiration in a northern temperate grassland. *Agricultural and Forest Meteorology* 130: 237–253.

Foken, T., and B. Wichura. 1996. Tools for quality assessment of surface based flux measurements. *Agricultural and Forest Meteorology* 78: 83–105.

Glenn, A.J., L.B. Flanagan, K.H. Syed, and P.J. Carlson. 2006. Comparison of net ecosystem CO_2 exchange in two peatlands in western Canada with contrasting dominant vegetation, *Sphagnum and Carex*. *Agricultural and Forest Meteorology* 140: 115–135.

Guan, Y.X., G.H. Liu, and J.F. Wang. 2001. Saline-alkali land in the Yellow River Delta: amelioration zonation based on GIS. *Journal of Geographical Sciences* 11: 313–320.

Guo, H.Q., A. Noormets, B. Zhao, J.Q. Chen, G. Sun, Y.J. Gu, B. Li, and J.K. Chen. 2009. Tidal effects on net ecosystem exchange of carbon in an estuarine wetland. *Agricultural and Forest Meteorology* 149: 1820–1828.

Heikkinen, J.E.P., V. Elsakov, and P.J. Martikainen. 2002. Carbon dioxide and methane dynamics and annual carbon balance in tundra wetland in NE Europe. *Russia. Global Biogeochemical Cycles* 16: 1115. doi:10.1029/2002GB001930.

Heinsch, F.A., J.L. Heilman, K.J. McInnes, D.R. Cobos, D.A. Zuberer, and D.L. Roelke. 2004. Carbon dioxide exchange in a high marsh on the Texas Gulf Coast: effects of freshwater availability. *Agricultural and Forest Meteorology* 125: 159–172.

Hirota, M., Y.H. Tang, Q.W. Hu, S. Hirata, T. Kato, W.H. Mo, G.M. Cao, and S. Mariko. 2006. Carbon dioxide dynamics and controls in a deep-water wetland on the Qinghai-Tibetan Plateau. *Ecosystems* 9: 673–688.

Houghton, R.A., and G.M. Woodwell. 1980. The flax pond ecosystem study: exchange of CO_2 between a salt marsh and the atmosphere. *Ecology* 61: 1434–1445.

Högberg, P., A. Nordgren, and G.I. Ǻgren. 2002. Carbon allocation between tree root growth and root respiration in boreal pine forest. *Oecologia* 132: 579–581.

Hsieh, C.I., G.G. Katul, and T.W. Chi. 2000. An approximate analytical model for footprint estimation of scalar fluxes in thermally stratified atmospheric flows. *Advances in Water Resources* 23: 765–772.

Kaimal, J.C., and J.J. Finnigan. 1994. *Atmospheric boundary layer flows: their structure and measurement*. Oxford: Oxford University Press. 289 pp.

Kathilankal, J., T. Mozdzer, J.D. Fuentes, P. D'Odorico, K.J. McGlathery, and J.C. Zieman. 2008. Tidal influences on carbon assimilation by a salt marsh. *Environmental Research Letters* 3: 6. 044010.

Larmola, T., J. Alm, S. Juutinen, P.J. Martikainen, and J. Silvola. 2003. Ecosystem CO_2 exchange and plant biomass in the littoral zone of a boreal eutrophic lake. *Freshwater Biology* 48: 1295–1310.

Li, S.N., G.X. Wang, W. Deng, Y.M. Hu, and W.W. Hu. 2009. Influence of hydrology process on wetland landscape pattern: A case study in the Yellow River Delta. *Ecological Engineering* 35: 1719–1726.

Lloyd, J., and J.A. Taylor. 1994. On the temperature dependence of soil respiration. *Functional Ecology* 8: 315–323.

Luo, X.X., and Z.Q. Xing. 2010. Comparative study on characteristics and influencing factors of soil respiration of reed wetlands in Yellow River Estuary and Liaohe River Estuary. *Procedia Environmental Sciences* 2: 888–895.

Nieveen, J.P., C.M.J. Jacobs, and A.F.G. Jacobs. 1998. Diurnal and seasonal variation of carbon dioxide exchange from a former true raised bog. *Global Change Biology* 4(8): 823–833.

Oechel, W.C., S.J. Hastings, G. Vourlitis, M. Jenkins, G. Riechers, and N. Grulke. 1993. Recent change of Arctic tundra ecosystems from a net carbon dioxide sink to a source. *Nature* 361: 520–523.

Polsenaere, P., E. Lamaud, V. Lafon, J.-M. Bonnefond, P. Bretel, B. Delille, J. Deborde, D. Loustau, and G. Abril. 2012. Spatial and temporal CO_2 exchanges measured by Eddy Covariance over a temperate intertidal flat and their relationships to net ecosystem production. *Biogeosciences* 9: 249–268.

Reichstein, W., J.D. Tenhunen, and O. Roupsard. 2002. Severe drought effects on ecosystem CO_2 and H_2O fluxes in three Mediterranean evergreen ecosystems: revision of current hypothesis? *Global Change Biology* 8: 999–1017.

Ruimy, A., P.G. Jarvis, D.D. Baldocchi, and B. Saugier. 1995. CO_2 fluxes over plant canopies and solar radiation: a review. *Advances in Ecological Research* 26: 1–68.

Ryan, M.G. 1991. Effects of climate change on plant respiration. *Ecological Applications* 1: 157–167.

Sabine, C.L., M. Heimann, P. Artaxo, D.C.E. Bakker, C.-T.A. Chen, C.B. Field, N. Gruber, C.L. Quere, R.G. Prinn, J.E. Richey, P.R. Lankao, J.A. Sathaye, and R. Valentini. 2004. *Current status and past trends of the global carbon cycle*. Washington: Island Press.

Saito, M., A. Miyata, H. Nagai, and T. Yamada. 2005. Seasonal variation of carbon dioxide exchange in rice paddy field in Japan. *Agricultural and Forest Meteorology* 135: 93–109.

Schedlbauer, J.L., S.F. Oberbauer, G. Starr, and K.L. Jimenez. 2010. Seasonal differences in the CO_2 exchange of a short-hydroperiod Florida Everglades marsh. *Agricultural and Forest Meteorology* 150: 994–1006.

Shi, P.L., X.M. Sun, L.L. Xu, X.Z. Zhang, Y.T. He, D.Q. Zhang, and G.R. Yu. 2006. Net ecosystem CO_2 exchange and controlling factors in a steppe–*Kobresia* meadow on the Tibetan Plateau. *Science in China Series D-Earth Sciences* 49: 207–218.

Syed, K.H., L.B. Flanagen, P.J. Carlson, A.J. Glenn, and K.E. Gaalen. 2006. Environmental control of net ecosystem CO_2 exchange in a treed, moderately rich fen in northern Alberta. *Agricultural and Forest Meteorology* 140: 97–114.

Van Dijk, A.I.J.M., and A.J. Dolman. 2004. Estimates of CO_2 uptake and release among European forests based on eddy covariance data. *Global Change Biology* 10: 1445–1459.

Webb, E.K., G.I. Pearman, and R. Leuning. 1980. Correction of flux measurements for density effects due to heat and water vapor transport. *Quarterly Journal of the Royal Meteorological Society* 106: 85–100.

Wickland, K., R. Striegl, M. Mast, and D. Clow. 2001. Carbon gas exchange at a southern Rocky Mountain wetland, 1996–1998. *Global Biogeochemical Cycles* 15: 321–335.

Wohlfahrt, G., M. Anderson-Dunn, M. Bahn, M. Balzarolo, F. Berninger, C. Campbell, A. Carrara, A. Cescatti, T. Christensen, S. Dore, W. Eugster, T. Friborg, M. Furger, D. Gianella, C. Gimeno, K. Hargreaves, P. Hari, A. Haslwanter, T. Johansson, B. Marcolla, C. Milford, Z. Nagy, E. Nemitz, N. Rogiers, M.J. Sanz, R.T.W. Siegwolf, S. Susiluoto, M. Sutton, Z. Tuba, F. Ugolini, R. Valentini, R. Zorer, and A. Cernusca. 2008. Biotic, abiotic, and management controls on the net ecosystem CO_2 exchange of European mountain grassland ecosystems. *Ecosystems* 11: 1338–1351.

Xie, T., X.H. Liu, and T. Sun. 2011. The effects of groundwater table and flood irrigation strategies on soil water and salt dynamics and reed water use in the Yellow River Delta, China. *Ecological Modelling* 222: 241–252.

Xu, L.K., and D.D. Baldocchi. 2004. Seasonal variation in carbon dioxide exchange over a Mediterranean annual grassland in California. *Agricultural and Forest Meteorology* 1232: 79–96.

Xu, M., and Y. Qi. 2001. Spatial and seasonal variations of Q_{10} determined by soil respiration measurements at a Sierra Nevadan forest. *Global Biogeochemical Cycles* 15: 687–696.

Yan, Y.E., B. Zhao, J.Q. Chen, H.Q. Guo, Y.J. Gu, Q.H. Wu, and B. Li. 2008. Closing the carbon budget of estuarine wetlands with tower-based measurements and MODIS time series. *Global Change Biology* 14: 1690–1702.

Yan, Y.E., H.Q. Guo, Y. Gao, B. Zhao, J.Q. Chen, B. Li, and J.K. Chen. 2010. Variations of net ecosystem CO_2 exchange in a tidal inundated wetland: coupling MODIS and tower-based fluxes. *Journal of Geophysical Research–Atmospheres* 115: D15102.

Zhang, G.S., R.Q. Wang, and B.M. Song. 2007. Plant community succession in modern Yellow River Delta, China. *Journal of Zhejiang University (Science B)* 8: 540–548.

Zhang, J.H., S.J. Han, and G.R. Yu. 2006. Seasonal variation in carbon dioxide exchange over a 200-year-old Chinese broad-leaved Korean pine mixed forest. *Agricultural and Forest Meteorology* 137: 150–165.

Zhang, T.T., S.L. Zeng, Y. Gao, Z.T. Ouyang, B. Li, C.M. Fang, and B. Zhao. 2011. Assessing impact of land uses on land salinization in the Yellow River Delta, China using an integrated and spatial statistical model. *Land Use Policy* 28: 857–866.

Zhao, L., J. Li, S. Xu, H. Zhou, Y. Li, S. Gu, and X. Zhao. 2010. Seasonal variations in carbon dioxide exchange in an alpine wetland meadow on the Qinghai-Tibetan Plateau. *Biogeosciences* 7: 1207–1221.

Zhou, L., G.S. Zhou, and Q.Y. Jia. 2009. Annual cycle of CO_2 exchange over a reed (*Phragmites australis*) wetland in Northeast China. *Aquatic Botany* 91: 91–98.